ACS OMEGA

Open Access

http://pubs.acs.org/journal/acsodf

Article

A Kinetic Approach to Synergize Bactericidal Efficacy and Biocompatibility in Silver-Based Sol−Gel Coatings

Thibaut Zwingelstein, Agathe Figarol,* Vincent Luzet, Maude Crenna, Xavier Bulliard, Alba Finelli, Julien Gay, Xavier Lefèvre, Raphaël Pugin, Jean-François Laithier, Frédéric Chérioux, and Vincent Humblot*

Cite This: *ACS Omega* 2024, 9, 24574−24583

Read Online

ACCESS | Metrics & More | Article Recommendations | Supporting Information

ABSTRACT: Silver ions are antimicrobial agents with powerful action against bacteria. Applications in surface treatments, as Ag^+-functionalized sol−gel coatings, are expected in the biomedical field to prevent contaminations and infections. The potential cytotoxicity of Ag^+ cations toward human cells is well known though. However, few studies consider both the bactericidal activity and the biocompatibility of the Ag^+-functionalized sol−gels. Here, we demonstrate that the cytotoxicity of Ag^+ cations is circumvented, thanks to the ability of Ag^+ cations to kill *Escherichia coli* (*E. coli*) much faster than normal human dermal fibroblasts (NHDFs). This phenomenon was investigated in the case of two silver nitrate-loaded sol−gel coatings: one with 0.5 w/w% Ag^+ cations and the second with 2.5 w/w%. The maximal amount of released Ag^+ ions over time (0.25 mg/L) was ten times lower than the minimal inhibition (MIC) and minimal bactericidal (MBC) concentrations (respectively, 2.5 and 16 mg/L) for *E. coli* and twice lower to the minimal cytotoxic concentration (0.5 mg/L) observed in NHDFs. *E. coli* were killed 8−18 times, respectively, faster than NHDFs by silver-loaded sol−gel coatings. This original approach, based on the kinetic control of the biological activity of Ag^+ cations instead of a concentration effect, ensures the bactericidal protection while maintaining the biocompatibility of the Ag^+ cation-functionalized sol−gels. This opens promising applications of silver-loaded sol−gel coatings for biomedical tools in short-term or indirect contacts with the skin.

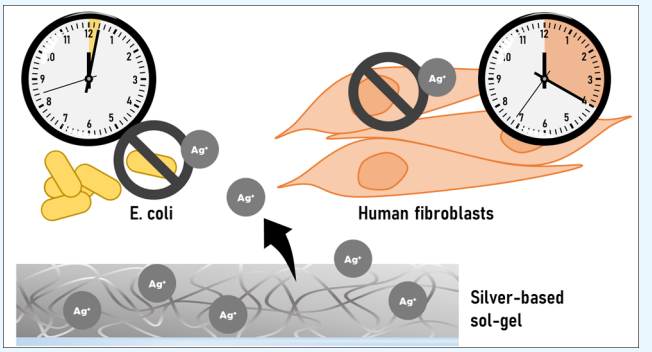

I. INTRODUCTION

Ag^+ ions and Ag-based compounds have been used for centuries as antimicrobial agents toward a large spectrum of bacteria, viruses, and even fungi, with different efficacies as a function of the targeted microorganism[1] over different forms such as colloid, suspension, powder, or gel.[2] Different materials can be chosen as a host matrix to stabilize Ag-based compounds as a surface coating: polymers, ceramics, or hybrid organic−inorganic materials. In the last category, coatings based on sol−gel chemistry are particularly interesting due to the wide range of microstructures that can be generated through the choice and ratio of precursors and of the drying and curing conditions. In particular, the density and porosity of the coating can be tuned, and the sol−gel materials can act as a reservoir of silver-based compounds, with a controlled release depending on its porosity.[3]

For conferring antimicrobial activity to sol−gel coatings, different approaches and different Ag^+ sources can be used. A first method consists of mixing the sol−gel solution with a silver salt ($AgNO_3$) before coating the mix on the desired surface. In a second approach, the silver salt can be reduced to form finely dispersed Ag^0 colloids either before or after coating on the surface by dipping the coating in a reducing solution. In a third approach, silver Ag^0 nanoparticles can be directly mixed with the sol−gel solution before coating the surface. In the cases of nanoparticles or colloids, the drawbacks are the rapid change of sol−gel coating properties, such as a drastic modification of the color and transparency or an alteration in the mechanical or protective properties, with low amounts of colloids or particles present at the surface of the coatings. The incorporation of $AgNO_3$ salt, on the other hand, barely modifies the initial properties of the coatings. The release of Ag^+ cations to the surface should, however, be properly controlled for bacteria contact killing. The kinetics of release through the sol−gel has not been quantified yet and is one of the topics of this study. Furthermore, the possible cytotoxic

Received: January 22, 2024
Revised: April 22, 2024
Accepted: April 25, 2024
Published: May 30, 2024

Scheme 1. Scheme of the Sample Preparation for the Sol−Gel Coating Consisting of a Preparation of the Base Sol−Gel Solution, the Addition of $AgNO_3$ in the Form of Powder, and the Dip-Coating Process on Glass Slides

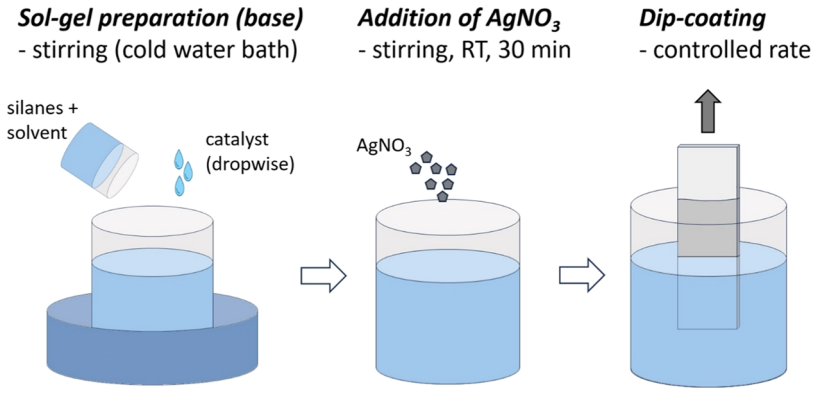

effect on human cells with regards to the bactericidal effect is still controversial.

The role of silver as an antimicrobial agent has been widely studied; however, its impacts on mammal and human cells should indeed be further addressed. This is a fairly common issue among the research against drug-resistance bacteria. The same physicochemical properties that give metal nanoparticles an antimicrobial potential[4] can lead to a worrying toxic impact on the human health.[5−7] Based on a literature review, only a few scientific articles considered both points when studying silver-loaded sol−gel coatings (see the Supporting Information).[8−12] In a review published by Simchi et al.,[8] it was stated that in given concentrations, silver was not toxic for human cells. The authors were referring to 3 articles to support this argument: the first one[13] did not contain any results on biocompatibility; in the second one,[14] no difference in cytotoxicity between the hydroxyapatite coating with or without Ag was observed, however, on extracts only and without a negative control; and finally, the third article[15] showed a significant decrease in cell viability after exposition to the hydroxyapatite coating containing 0.21−0.45 wt % Ag from $AgNO_3$ mixed with hydroxyapatite and coated on titanium substrates with microarc oxidation. The other articles studying both the bactericidal and the cytotoxicity properties of Ag-containing sol−gels gave contradictory results, with two showing a significant toxicity and two showing no toxicity. Zhang et al.[12] used Ag nanoparticles with polytetrafluoroethylene as a sol−gel coating and studied both the impacts on bacteria and mammal cells. They showed that it was efficient against *Escherichia coli* (bacterial biomass accumulation down to 10% after 1 day and 50% after 7 days). Nevertheless, the authors expressed concerns for local toxicity as they observed a decrease in mouse fibroblast activity (MTT assay) and morphological observations related to cell stress: loss of their typical spindle shape, cytoplasmic condensation or shrinkage, and rounded cells. Jaiswal et al.[10] studied silver nitrate and silver coumarin complex-doped sol−gel coatings for their bactericidal effects on *Staphylococcus aureus* and *Enterobacter cloacae* and cytotoxic impacts on human keratinocytes. Unfortunately, the bactericidal efficiency seemed to be linked to a cytotoxic effect. Rahmani et al.[11] assessed a bioactive glass doped with silver oxide: $60SiO_2$-$(31-x)$ $CaO-4P_2O_5-5Li_2O-xAg_2O$, and on the contrary, showed no decrease in cell viability on mouse osteoblasts while exhibiting a bactericidal activity against *E. coli*. Likewise, Aksakal et al.[9] observed no decrease in human osteoblast-like cells exposed to glass loaded with selenium and 5−20 wt % $AgNO_3$. The differences in the matrix chemistry, cell and bacteria types, and expression of the Ag concentrations hinder the comparisons between the rare studies on the subject.

The literature is more abundant on silver potential cytotoxicity as a free ion form, not embedded in a sol−gel matrix. The present study will focus on mammal and human fibroblasts as a model for dermal and connective tissues. There is a weak consensus on biocompatible doses about 0.5−1 mg/L Ag^+.[16−18] However, while below 1 mg/L, there might be no decrease in fibroblast viability, other signs of toxicity are present. At 0.45 mg/L, a decrease in protein expression and an impairment in DNA synthesis can be observed.[17] Between 0.5 and 1 mg/L, a significant increase in the production of reactive oxygen species can be initiated.[18]

These findings highlight the crucial importance of a toxicity assessment on human tissues while developing Ag^+-based bactericidal sol−gel coatings. In this study, we have developed a new strategy to prevent the cytotoxicity of Ag^+ cations while maintaining their bactericidal property. This strong achievement is due to the ability of Ag^+ cations to kill bacteria much faster than that of human dermal cells. This approach paves the way for applications of silver-loaded sol−gel coatings for biomedical materials in short-term or indirect contacts with the skin such as some medical tools and utensils.

The physicochemical properties of two sol−gel coatings containing silver were first assessed. Their impacts on a model bacteria, *E. coli*, and normal human dermal fibroblasts (NHDFs) were investigated with conventional dose-dependent and innovative time-dependent approaches. This original perspective, based on kinetic control of the biological activity of Ag^+ cations instead of a concentration effect, could ensure bactericidal protection while maintaining the biocompatibility of the sol−gels.

II. MATERIALS AND METHODS

II.I. Chemicals. $AgNO_3$, phosphate buffer saline (PBS), tetraethylorthosilicate, isobutyltrimethoxysilane, nitric acid, ethanol, isopropanol, ciprofloxacin, ampicillin, chloramphenicol, streptomycin, penicillin, Triton X-100, microbiological agar, Luria−Bertani broth, bovine gelatin, cell medium (Dulbecco's modified Eagle's medium (DMEM), 2% glutamine), trypsin-EDTA (0.25−0.02%), trypan blue, and fetal bovine serum (FBS) were purchased from Merck, Fisher, Gelest, and TCI Chemicals and used without any further treatment.

https://doi.org/10.1021/acsomega.4c00726
ACS Omega 2024, 9, 24574−24583

II.II. Sol−Gel. *II.II.I. Sol−Gel Formulation.* The base sol−gel formulation was composed of tetraethylorthosilicate (TEOS, 17.8 mL), isobutyltrimethoxysilane (3.6 mL), ethanol as a solvent (10.7 mL), and acidified water (2% vol HNO_3; 9.4 mL) as the catalyst. A 100 mL beaker was placed in a cold water bath, as the sol−gel hydrolysis reaction is exothermic. Isobutyltrimethoxysilane, with a saturated bond, was added to slightly decrease the sol−gel network density and avoid cracking of the sol−gel layer. The components were added successively, with the acidified water added at last, dropwise. Powdered silver nitrate (0.5 or 2.5 wt % in Ag) was then added to the solution under continuous stirring. Stirring was pursued during 30 min to ensure a perfect dissolution. The solution turned slightly gray.

II.II.II. Sample Coating. Glass slides (microscope glass, DWK Life Science) were used as a substrate. Before sol−gel deposition, the slides were cleaned in isopropyl alcohol for 10 min under sonication. Deposition was carried out by dip-coating using the KSV Nima medium (Biolin Scientific, Finland). The glass slides were dipped into the sol−gel solution for a few seconds and removed at a constant speed of 100 mm/min. The sol−gel coating route is represented schematically in Scheme 1. After coating, the slides were allowed to dry for 10 min. The coated slides were then placed into an oven, preheated at 60 °C, for curing. The temperature was then raised to 100 °C for 1 h and cooled again to 60 °C before removing after 1 additional hour. The glass slides were then cut into pieces of 0.5 cm x 0.5 cm by laser cutting for further tests. The thickness of the coating was measured using a stylus profilometer (Burker Dektak XT) and it reached 0.61 μm for a sol−gel without $AgNO_3$, and 0.65 and 0.69 μm, respectively, for a sol−gel with 0.5 and 2.5 wt % Ag. The morphology of the sol−gel coatings was investigated by scanning electron microscopy (Figure S1). No significant changes in deposit morphology were observed based on the amount of silver content in the sol−gel.

The chosen $AgNO_3$ concentration range (0.5 and 2.5 wt %) was set, for the lower limit, to guarantee sufficient release from the coating (as explained below) and, for the upper limit, to form a homogeneous coating on the glass. Above this limit, the coating gradually got an unwanted gray color.

II.III. Preparation of $AgNO_3$ Solutions. $AgNO_3$ solutions for microbiology experiments were freshly prepared in Milli-Q water at an initial Ag^+ concentration of 800 mg/L and diluted as needed for the different in vitro experiments.

II.IV. Inductively Coupled Plasma Atomic Emission Spectrometry (ICP-AES) Experiments. *II.IV.I. Release Experiments.* Glass slides loaded with sol−gel, sol−gel 0.5 and 2.5% Ag^+ cations, were suspended in 5 mL of PBS at 30 °C and stirred at 90 rpm. For each indicated time, the whole solution was recovered and replaced by 5 mL of fresh PBS. Ag^+ cation concentrations in the solution were determined using inductively coupled plasma atomic emission spectrometry (ICP-AES). Standard control was achieved by analyzing a calibrated solution at 5 mg/L.

II.IV.II. Ag^+ Cation Incorporation within Bacteria. Two $\times 10^6$ CFU/mL of *E. coli* were put in contact in 10 mL of $AgNO_3$ solution in PBS at a concentration of 5 mg/L Ag^+ cations for 30 min at 30 °C under 90 rpm agitation. The control solution was 10 mL of PBS with $AgNO_3$ at a concentration of 5 mg/L Ag^+ cations.

II.V. Bacteria Culture. *E. coli* ATCC 25922 were stocked at −80 °C in glycerol stock. The inoculum was prepared by first growing a solid culture on biological agar (15 mg/L) + LB (20 mg/L) Petri dishes incubated overnight at 30 °C. Thus, liquid cultures were carried out by recovering 1 colony from the solid growth Petri dish and inoculated in 5 mL of LB media at 20 mg/L and cultured overnight at 30 °C under 90 rpm agitation.

II.V.I. Contact Killing. Exponentially growing *E. coli* in LB was harvested by centrifugation (5000*g*, 5 min, 25 °C), washed twice with PBS, and suspended in PBS to obtain a concentration of 10^9 CFU/mL. 50 μL portion of this bacterial suspension was spread onto 89 mm Petri dishes filled with agar + LB media, using an Interscience EasySpiral automatic seeder. Thus, glass slides were deposited face-down on the freshly incubated Petri dishes by avoiding the creation of air bubbles. After overnight incubation at 30 °C, the photos were recorded using an Interscience colony counter Scan 300. Controls were run without the loading of $AgNO_3$ in the sol−gel matrix.

II.V.II. Minimal Inhibition Concentration (MIC) and Minimal Bactericidal Concentration (MBC) Experiments. MIC values toward *E. coli* were determined using the 2-fold dilution method. Experiments were performed in 96-well microplates in triplicate in culture media (LB), with an initial bacterial concentration of approximately 10^6 CFU/mL. The highest concentrations were prepared according to the following: $AgNO_3$ in distilled water at an Ag concentration of 320 and 64 mg/L resulting in concentrations in the first well of 80 and 16 mg/L, respectively. After overnight incubation at 30 °C, MIC values were determined as the lowest concentration of the compound with no visible bacterial growth. Sterility control (culture broth only), growth control (culture broth with bacteria), and death control (culture broth with bacteria and ethanol: H_2O v/v 70/30) assessed the quality of each experiment.

E. coli MBC determination was performed by measuring the 96-well plates in a ultraviolet (UV) spectrophotometer with the optical density (OD) at a 620 nm wavelength, after determination of the MIC values and resuspension of the bacterial pellets. MBC values were determined when the OD value was less than 0.001× the OD of the control growth.

II.V.III. Kinetics of Bactericidal Action. Exponentially growing *E. coli* in LB was harvested by centrifugation (5000*g*, 5 min, 25 °C), washed twice with PBS, and suspended in PBS to obtain a concentration of 10^6 CFU/mL. Ten mL of this bacterial suspension was incubated at 30 °C under 90 rpm agitation. At each time of the assay (0, 5, 10, 15, 20, 25, 30, 40, 50, 60, 75, 90, 120, 150, 180 min), 100 μL of the solution was recovered and diluted 10 and 100 times in PBS. Thus, 50 μL of both dilutions were spread onto 89 mm Petri dishes filled with LB + agar (20 + 15 g/L, respectively), using an Interscience EasySpiral automatic seeder. After overnight incubation at 30 °C, the CFUs were enumerated and recorded using an Interscience colony counter Scan 300. Controls were run without the loading of $AgNO_3$ in the bacterial solution.

Ag^+ cation concentrations were chosen as a function of MIC values at MIC/2 and MIC, i.e., 1.25 and 2.5 mg/L, respectively.

II.V.IV. Evaluation of Incorporated Ag in Bacteria. 10^6 CFU/mL *E. coli* were put in contact in 10 mL of $AgNO_3$ solution in PBS at a concentration of 5 mg/L Ag^+ cations for 30 min at 30 °C and 90 rpm agitation. Thus, bacteria were centrifuged and separated from the supernatant, and both resulting solutions were analyzed by ICP-AES to determine the Ag^+ cation concentration. Four solutions were analyzed: a

https://doi.org/10.1021/acsomega.4c00726
ACS Omega 2024, 9, 24574−24583

control at 5 mg/L in Ag (S1), the mix bacteria + $AgNO_3$ (S2), and finally a solution with the centrifugated bacteria (S4) vs its supernatant (S3).

II.VI. Cell Culture. NHDFs from the abdomen were graciously provided by Dr. Céline Viennet from UMR 1098 RIGHT INSERM EFS UBFC. Cells were cultured in Dulbecco's modified Eagle's medium (DMEM) with 2% glutamine, complemented with 10% fetal bovine serum (FBS) and 1% penicillin-streptomycin (100 U/mL and 0.1 mg/mL, respectively), and incubated at 37 °C with 5% CO_2 in a humidified atmosphere. The cells were passaged every 3 or 4 days and seeded at 10,000 cells/cm^2 for culture maintenance.

II.VI.I. Cytotoxicity Assays. For the assessment of Ag^+ cation toxicity from free $AgNO_3$ powder, 28,000 cells/cm^2 in DMEM without FBS were seeded in 96-well plates (90,000 cells/mL, 100 μL/well). The cells were incubated for 24 h for optimum adhesion and then exposed to 0−6 mg/L Ag^+ cation equivalent (addition of 100 μL/well of concentrated $AgNO_3$ solutions). For the assessment of Ag^+ cation toxicity from the sol−gel film release, 30 000 cells/cm^2 in DMEM without FBS were seeded in 24-well plates on top of 1 cm^2 sol−gel samples (60,000 cells/mL, 1 mL/well, 1 sample/well, no sample in control wells). For both experiment types, the cells were then incubated for 24 h at 37 °C and 5% CO_2 before microscopic observations and cytotoxicity assays.

The cell viability was evaluated using an MTT assay (3-(4,5-dimethylthiazol-2-yl)-2,5-diphenyltetrazolium bromide). Cells in the positive control well were exposed to 10% v/v Triton X-100 for 30 min. The MTT kit (Merck, reference 11465007001) was used according to the manufacturer's recommendations. Basically, a 10% v/v MTT labeling reagent was added into the cell supernatant; after a 4 h incubation at 37 °C, 5% CO_2, a 100% v/v stabilization solution was then added. The absorbance was read at 600 nm after an overnight incubation at 37 °C and 5% CO_2 (Clariostar plate reader, BMG Labtech).

Before the MTT assay, 10 μL of cell supernatants were collected and transferred to a new 96-well plate to assess cell necrosis by measuring LDH (lactate dehydrogenase) release. The LDH kit (Merck, MAK380) was used according to the manufacturer's recommendations. Briefly, 100 μL of LDH mix reagents were added to 10 μL of the supernatant. After 30 min of incubation at room temperature, protected from light, 10 μL of the stop solution was then added. The absorbance was then read at 450 nm (Clariostar plate reader).

LDH cytotoxicity assay was conducted for $AgNO_3$ free powder. Black 96-well plates with transparent bottoms coated with porcine gelatin (1% m/v) were used for this assay. Cells in the positive control well were exposed to 70% v/v ethanol for 5 min. The live−dead kit (Merck, CBA415) was used according to the manufacturer's recommendations. After removal of the supernatants, 100 μL of the live−dead mix was added per well (0.4 μL/mL calcein, 1.7 μL/mL propidium iodide, 0.4 μL/mL Hoechst, in 50% v/v DMEM without FBS, and 50% v/v PBS). After a 30 min incubation at 37 °C, 5% CO_2, the fluorescence was read at 490/515, 535/617, and 361/486 nm (Ex/Em, Clariostar plate reader), and pictures were taken with a fluorescent microscope (Axio observer, Zeiss).

II.VI.II. Kinetics of the Cytotoxicity. The same experimental conditions were used to prepare the cells for the toxicity assay of $AgNO_3$ free powder and for the kinetics assay with only 3 concentrations: 0, 1.25, and 2.5 mg/L Ag^+ cations (equivalent to MIC/2 and MIC). For the kinetics assay, however, the cells were observed directly after exposure to $AgNO_3$. Pictures were taken with a wide field microscope, at ×100 magnification, every 5 min from t0 to t30 min, every 10 min from t30 to t60 min, every 15 min from t60 to t90 min, and every 30 min from t90 to t180 min. Image analyses were carried out by two different experiments with ImageJ software and the cell counter plugin. Cells presenting a healthy morphology (adherent, slender fibroblasts) were counted separately from cells presenting an apoptotic morphology (round, detached, blebbing). Viability results were calculated as the average number of healthy cells divided by the total number of cells (>60 cells per images, three images per condition, 3 independent experiments).

II.VII. Statistical Analyses. Three independent experiments were carried out for each assay in triplicate, except when precised. Error bars represent standard deviations. Two by two comparisons of results (sample versus control) were performed. Student's t test first assessed the variance similarity of the two groups. The p values were then calculated using the two-tailed Fisher test. A difference was considered significant if * $p < 0.05$, ** $p < 0.01$, or *** $p < 0.0005$.

As shown in Figure 1, standard deviations were obtained from measurements carried out on the standard solution, ending up to a 1.4% deviation applied to all ICP-AES data.

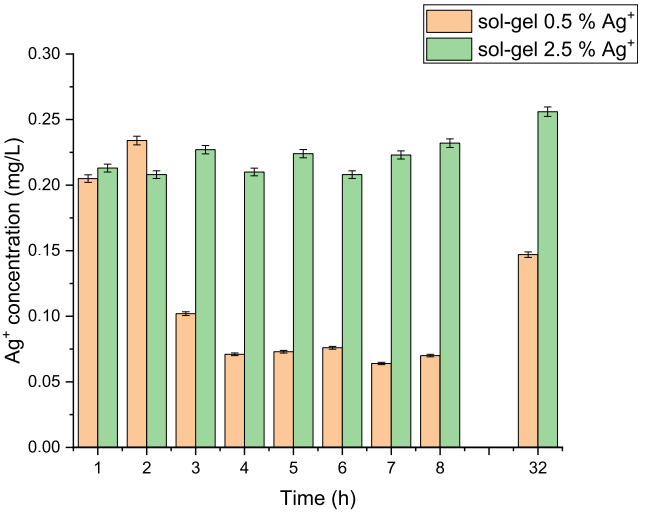

Figure 1. Ag^+ release in PBS at 30 °C for sol−gel coatings loaded with 0.5 and 2.5 mass % Ag.

III. RESULTS

Experiments were performed to investigate the potential release of Ag^+ cation bactericidal moieties from the sol−gel films loaded with $AgNO_3$. The results are presented in Figure 1, showing ICP-AES measurements of the Ag^+ cation concentration in solution after immersion of Ag^+-loaded sol−gel-coated glass slides in PBS solutions. Time-lapse assays were performed successively for 1 h of immersion, repeated 8 times (from 1 to 8 h in the x-axis), and a further 24 h immersion was performed (32 h in the x-axis). For each considered time, the PBS solution was renewed before the next time slot.

For the 0.5% Ag^+-loaded sol−gel film, after an initial release close to 0.20 mg/L for the first 2 hours, the release amount dropped to 0.10 mg/L for the next 6 h assays. The further 24 h immersion led to an average concentration of 0.15 mg/L. For

https://doi.org/10.1021/acsomega.4c00726
ACS Omega 2024, 9, 24574−24583

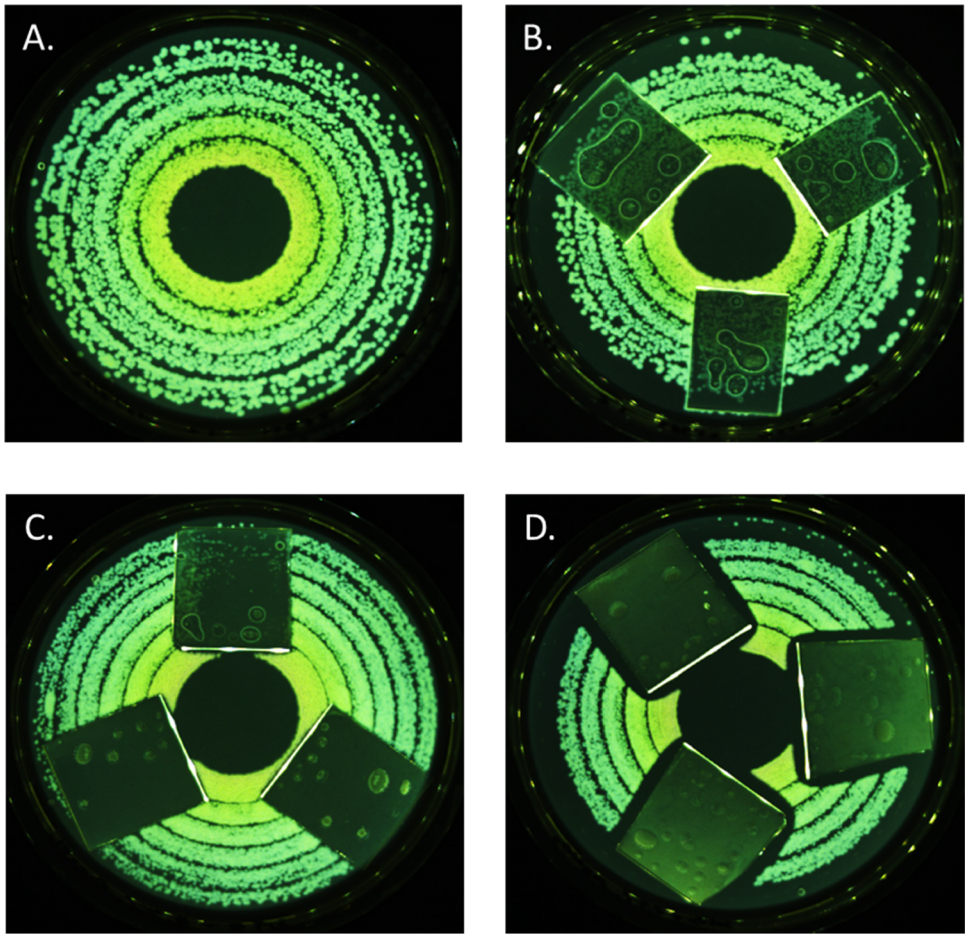

Figure 2. Petri dishes spread with 50 μL of an *E. coli* inoculum at 10^9 CFU/mL. (A) Growth control; (B) sol−gel matrix, 0% $AgNO_3$; (C) sol−gel 0.5% $AgNO_3$; and (D) sol−gel 2.5% $AgNO_3$. % $AgNO_3$ is expressed as mass % of Ag^+ cations within the sol−gel matrix.

the 2.5% Ag^+-loaded film, the measured concentrations were comprised between 0.20 and 0.25 mg/L, regardless of the number of successive immersions and of the length of the immersion (1 or 24 h). These results showed, first, that the films acted as Ag^+ cation reservoirs able to release active product in solution as a function of time. Second, one can note that the 0.5% films start to be depleted after 2 immersions of 1 h. Furthermore, even after 24 h of immersion, the initial concentration of around 0.20 mg/L was not reached anymore, confirming the depletion of the matrix, showing that the release was not driven by time or kinetics. Concerning the 2.5% loaded film, the released quantities were stable, regardless of the numbers of immersion or the duration of the immersion. This result led to the conclusion that an ionic and/or solubility equilibrium was reached upon the release of Ag^+ cations in the PBS solution, limiting the maximum quantity of Ag^+ cations in solution.

The present study focused on *E. coli*. Experiments were carried out to determine the minimal inhibition concentration (MIC) that demonstrates the lowest level of the antimicrobial agent that inhibits growth and the minimal bactericidal concentration (MBC) tests that demonstrate the lowest level of the antimicrobial agent resulting in microbial death. Tables S1, S2 and Figure S2 present the MIC/MBC obtained in vitro for the *E. coli* ATCC 25922 strain. One can see that from these data, MIC and MBC were evaluated at 2.5 and 16 mg/L, respectively, showing therefore greater antibacterial activities than commonly used antibiotics, thus reinforcing our choice of Ag^+ cations for bactericidal coatings.

The antimicrobial properties of Ag^+ cations may lead to side effects for human cells. The cytotoxicity of Ag^+ cations toward NHDFs was assessed after 24 h exposures. The results can be found in the Supporting Information (Figure S3). From 0.75 mg/L, a dose-dependent decrease in cell viability and an increase in cell necrosis were observed. Over 1 mg/L, however, the cytotoxicity reached a plateau with less than 40% cells remaining viable, while no or scarce necrosis was noticed. Microscopic observations confirmed a decrease in the number of live cells after exposure to Ag^+ cations (almost no live cells stained with calcein, visible above 1.5 mg/L). The live−dead kit uses propidium iodide to label dead cells, which stains only the necrotic cells. Again, scarce stained necrotic cells were observed, while observation before staining showed a morphology typical from apoptotic cells (round, blebbing, and detached). Ag^+ cations seemed thus to induce apoptosis at concentrations higher than 0.75 mg/L. The observed levels of released Ag^+ cations from the sol−gel coating after 24 h in a row (data named 32 h) (Figure 1) show a maximum concentration of released Ag^+ of 0.25 mg/L, which is half of the lower tested dose (0.5 mg/L, Figure S3A) and therefore should not endanger those human cells within the time frame.

To evaluate the bactericidal efficiency of the sol−gel coatings loaded with $AgNO_3$, contact killing assays were performed on agar Petri dishes previously inoculated with 50

https://doi.org/10.1021/acsomega.4c00726
ACS Omega 2024, 9, 24574−24583

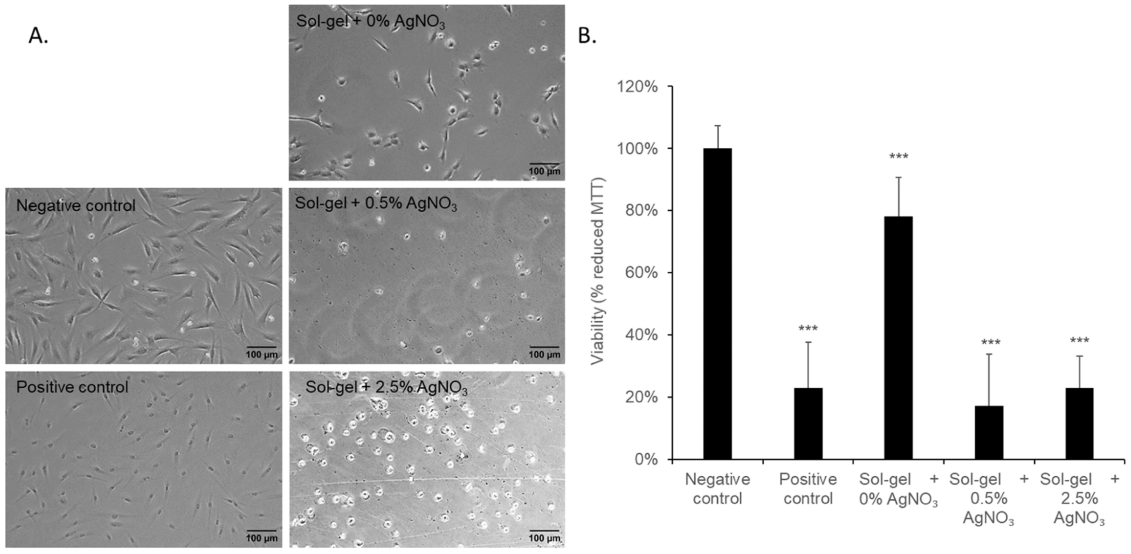

Figure 3. Cytotoxicity of the sol−gel films loaded with 0.5 or 2.5% $AgNO_3$ (i.e., 0.5 or 2.5 wt % Ag^+). (A) Microscopic observations of the fibroblasts after a 24 h growth on the sol−gel films or in a culture well without (negative control) or with 10% Triton X-100 (positive control). (B) Fibroblast viability after 24 h, expressed as percentages of reduced MTT salt compared with the negative control (*** $p < 0.0005$).

μL of *E. coli* bacteria at 10^6 CFU/mL, as shown in Figure 2A. Sol−gel films with and without Ag^+ loadings were deposited on the inoculated Petri dishes, and after overnight incubation (e.g., 16 h) at 30 °C, the evaluation of the bacterial growth was carried out. The bare sol−gel matrix without $AgNO_3$, as shown in Figure 2B, did not show any bactericidal effect as one can notice the presence of bacterial colonies under the glass slide. On the contrary, once the sol−gel matrix was loaded with $AgNO_3$, differences were observed, as shown in Figure 2C,D. First, it can be underlined that under the glass slides, no bacterial colonies were observed, suggesting contact killing or at least an inhibition growth of inoculated bacteria upon contact with the $AgNO_3$ sol−gel coatings. Moreover, for the sol−gel films loaded with 2.5% Ag^+ (Figure 2D), an inhibition growth halo is observable in the areas surrounding the coated glass slides, clearly suggesting a migration of the bactericidal products, i.e., Ag^+ compounds, hence suggesting the release of the products from the sol−gel films.

However, from the results shown in Figure 2, a release concentration within the range of 0.15−0.25 mg/L Ag^+ cations (Figure 1) seems to be enough to have an effective bactericidal effect, while in vitro MIC/MBC experiments (Table S1) highlight the fact that at least a concentration of 2.5−16 mg/L is required to observed the first bactericidal effect toward the same *E. coli* strain. This factor of 10× is quite surprising and could be explained by the method used for the ICP-AES release experiments. In fact, it was suggested that the highest release concentration is obtained once the solubility equilibrium is reached. This suggests that an external factor could either change the solubility value or decrease the Ag^+ concentration within the solution. This last point would end up with the sol−gel reservoir liberating more Ag^+ in solution to again reach the equilibrium.

In this purpose, we have designed a simple experiment to elucidate the fact that a release concentration of 10 times less than the MIC value was nonetheless able to show a bactericidal effect. Results are presented in Figure S4, showing both control solutions S1 and S2 as well as sample solutions S3 and S4. As expected, both S1 and S2 solutions had a concentration in Ag^+ cations close to the initial concentration, i.e., 5 mg/L, with 5.040 and 4.900 mg/L, respectively. Analyses of the solutions S3 and S4 after separation also showed very interesting results; after 30 min, more than 90% of the Ag^+ cations were present in the bacteria (S4, $C°_{Ag}$ = 4.510 mg/L), while only 10% of Ag^+ cations remained in the supernatant (S3, $C°_{Ag}$ = 0.478 mg/L), with the addition of S3 + S4 (4.988 mg/L) being almost equal to the initial concentration of 5 mg/L.

Based on this experiment, it seems clear that upon contact for 30 min between *E. coli* and $AgNO_3$ solution, 90% of the Ag^+ cations were incorporated with the bacteria, therefore depleting the concentration of free Ag^+ in the solution resulting in the ionic and/or solubility equilibrium to be disturbed. Keeping in mind this conclusion, this means that for the contact killing experiments presented in Figure 2, and performed during 16 h, after release of the initial 0.15−0.25 mg/L Ag^+ cations, the rapid incorporation of Ag^+ cations within *E. coli* bacteria enables the sol−gel reservoir to release more Ag^+ cations in the solution, potentially reaching concentration values close to the in vitro MIC/MBC values, thus explaining the bactericidal effect and inhibition halo observed for both sol−gels loaded with 0.5 and 2.5% Ag^+ cations.

Concomitantly, this meant that even if the measured released concentrations of Ag^+ cations from the sol−gel film were under the limit of cytotoxicity in mammal cells (Figures 1 and 3), the potential incorporation of Ag^+ cations within the cells could enhance more releasing from the sol−gel reservoir, thus decreasing the expected biocompatibility. Assays were carried out to assess the fibroblast response after a 24 h growth on the sol−gel surfaces. The cells displayed changes in the morphology after exposure to the sol−gels (Figure 3A). The bare sol−gel induced a reduced cell growth, with some round-shaped fibroblasts, which were signs of a moderate cytotoxicity. Once loaded with 0.5 or 2.5% Ag^+, the sol−gel seemed to impair the cell adhesion or to lead to a strong cytotoxicity as all cells were rounded, blebbing and for most of them, detached from the surface. The quantitative viability assay (potency for the mitochondrial reduction of MTT) is in line with these observations (Figure 3B). The bare sol−gel was responsible for a slight decrease in the viability to 78 ± 13, which remains over

https://doi.org/10.1021/acsomega.4c00726
ACS Omega 2024, 9, 24574−24583

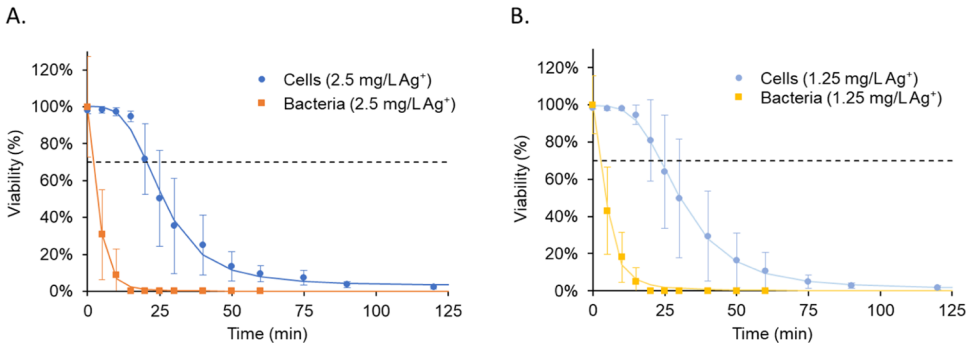

Figure 4. Kinetics of the viability decrease after exposure of cells (blue dots) or bacteria (yellow squares) to (A) 2.5 mg/L or (B) 1.25 mg/L Ag^+ cations from $AgNO_3$ (corresponding to the MIC and MIC/2). Three independent experiments in triplicate were carried out for the cell kinetics and two in triplicate for the bacteria kinetics.

the 70% considered the standard viability expectation.[19] Ag^+ cations contained in the loaded sol−gel induced, however, a significant decrease in viability, down to 17 ± 17 and 23 ± 10% for 0.5 and 2.5% Ag^+, respectively. To check whether this effect was due to a possible release of silicon present in the coating, ICP-AES analyses were carried out following the same parameters as for Ag^+ cations, this time focusing on silica leaching. The results showed a limited release of silica over time (between 0.05 and 0.2 ppm), attesting to the stability of the sol−gel layer. By changing either the curing conditions or the sol−gel composition to form a denser sol−gel network, this release can be suppressed (or below the limit of detection). The results of the LDH assay can be found in the Supporting Information (Figure S5). As for the assessment of the free $AgNO_3$ powder, Ag^+ loaded into the sol−gel did not seem to lead to necrosis but rather apoptosis. Regarding those three result groups, the hypothesis of the sol−gel acting as a reservoir seemed to be confirmed.

This set of experiments has demonstrated the difficulty to find a thermodynamic range for which the Ag^+ cation bactericidal protection would be achieved while maintaining the biocompatibility of the sol−gel. Could, however, a kinetic range be possible? The bacteria and cells were once again exposed to Ag^+ cations at the MIC and MIC/2 (2.5 and 1.25 mg/L, respectively) (Figure 4, and microscopy observations shown in Figure S6). As expected, the bacterial viability dropped significantly in a very short time, while the cell response kinetics was slower. A decrease to 70% of viability was observed after 20.6 min for cells and 2.7 min for bacteria exposed to 2.5 mg/L Ag^+ cations (Figure 4A) or after 23.6 min for cells and 3.1 min for bacteria exposed to 1.25 mg/L Ag^+ cations (Figure 4B). The sol−gel loaded with Ag^+ cations could thus lead to a bactericidal effect 8−18 times faster than a toxic response toward mammal cells.

IV. DISCUSSION

It is widely acknowledged that materials, such as sol−gel materials containing silver (as metal or cations), demonstrate antibacterial properties. Furthermore, chemically durable materials that release Ag^+ cations gradually over an extended period of time are sought for medical applications. In comparison to the use of standard antibiotics, Ag^+ cations have shown significant bactericidal efficacy without the potential development of antibiotic resistance.

Although the mechanism of the bactericidal action of Ag-based compounds or Ag^+ cations remains unclear, a few hypotheses have emerged in the recent literature. A common consensus suggests that exposure to Ag^+ cations disrupts the bacterial membrane, leading to the leakage of cytoplasm and intracellular contents.[2,20] This membrane disruption is often attributed to the strong interactions of Ag^+ cations with the constituents of bacterial membranes, primarily through interactions with thiol groups of membrane enzymes or proteins.[21]

Here, the concentrations at which free Ag^+ cations from $AgNO_3$ impact fibroblast viability (over 0.75 mg/L) align with the literature consensus presented in the introduction.[16−18] These concentrations vary, depending on experimental conditions, such as the chosen serum percentage in the medium. In our experiments, a serum-free medium was used, potentially overestimating the toxicity. However, the literature indicates deleterious cell responses at lower exposure doses, particularly at higher serum concentrations.[17]

Furthermore, minimum inhibitory concentration (MIC) and minimum bactericidal concentration (MBC) doses for bacteria were at least three times higher than the toxic doses observed for fibroblasts. Thus, even in the case of potential overestimation, it appears unlikely to find a concentration where Ag^+ cations inhibit bacterial growth while remaining biocompatible for human cells over a 24 h period. Direct contact assays were selected to assess the bactericidal and cytotoxic activity of Ag^+ cation-loaded sol−gel surfaces. Although the study of extracts from material releases is accepted by regulations on medical devices' biocompatibility,[22] it can underestimate material toxicity and lead to nonpertinent predictions of surface interactions with human tissues.[23] Similarly, the standard viability limit is set at 70%. While a 30% decrease in viability may already suggest a significant impact in vivo, such standards are essential for the standardized biological assessment of a material. As mentioned in the introduction, the release of Ag^+ from loaded sol−gels has been scarcely investigated in the literature[8,24] and comparing one study to another is challenging due to the substantial differences in materials.

In a study by Rahmani et al.,[11] a release of 0.2 mg/mL Ag^+ cation was observed after 1 day, increasing to 0.4 mg/L after 7−14 days from a sol−gel-derived quaternary bioactive glass with a composition of 60% SiO_2, 31% CaO, 4% P_2O_5, and 5% Li_2O (mol %). Another study by Luo et al.[25] focused on the release of the Ag^+ cation from a borate glass doped with 0.75, 1.0, and 2.0 wt % Ag_2O. The first two materials released up to 1 and 1.3 mg/L Ag^+ cations, respectively, and the third one released up to 2.5 mg/L Ag^+ cations during 48 h, with a significant decrease observed from 48 h to 1 week. These

https://doi.org/10.1021/acsomega.4c00726
ACS Omega 2024, 9, 24574−24583

examples underscore that variations in materials impact the release rate, plateau, and reservoir capacity of sol−gel coatings, thereby influencing their bioactivity. In our study, we have illustrated that the developed sol−gel matrix demonstrates a release of Ag^+ cations ranging from 0.15 to 0.25 mg/L. These values are significantly lower than those reported in the literature, as mentioned above. This difference can be attributed to the nature of the sol−gel matrix, which is effectively cross-linked due to the precise adjustment of the tetraethylorthosilicate/isobutyltrimethoxysilane ratio as well as the method to provide thin films onto glass slides (refer to the Materials [TC3]and Methods section for details).

The studied sol−gel surfaces released 0.15−0.25 mg/L Ag^+ cations, so 10 times lower than the MIC for *E. coli*, but showed nonetheless a bactericidal effect. ICP-AES backed up the hypothesis of the sol−gel acting as a reservoir, while the Ag^+ cations were internalized by bacteria. A similar mechanism is expected for fibroblasts. The results showed that apoptosis was surely the main cell death pathway after exposure to the Ag^+ cations. Apoptotic cores retain membrane integrity, and if internalized, the Ag^+ cations should be kept from being released into the medium. The same equilibrium displacement could occur as for the bacteria and induce Ag^+ cations to release from the sol−gel matrix. This finding is, at least partly, supported by the literature. Cell exposition to silver ions has indeed been reported as a cause of apoptosis[26,27] with an internalization of the Ag^+ cations in lysosome-like vehicles, and bounding to collagen fibers.

Rare are studies focusing on the kinetics of bacteria and cell killing with silver ions. Most of the assessments on mammal cells are carried out after 24 h, as we first did, respecting this standard. Zhan et al.[28] have however shown than Ag^+ cations were toxic for fibroblasts as soon as 30 min at 5.4 mg/L. Our results confirmed the considerable speed of the cytotoxicity mechanisms of Ag^+ cations against *E. coli*, 8−18 faster than against fibroblasts. Considering this, the competition between bacteria and cell internalization should be in favor of bacteria and reinforce the time delay between both toxic responses, enabling the use of this surface chemistry for bactericidal applications with short contacts with human skin. As for chemical disinfectants such as hypochlorite and phenolics, long-term contact with human tissues should be avoided. However, contrary to the current hospital disinfectants, the coated material itself can act as an antimicrobial agent. There is no need for repeated application of the disinfectants. This could be interesting for objects with frequent, brief, or indirect contacts with biological tissues. The silver-loaded sol−gel could be a supplementary tool in the complex strategies for disinfection in healthcare.[29]

V. CONCLUSIONS

The examined silver-loaded sol−gel coatings consistently released Ag^+ cations at constant concentrations. Despite the release concentrations being below toxic levels for bacteria or human skin cells, both bactericidal action and cytotoxicity were observed with the Ag^+ cation-loaded sol−gel coatings. The internalization of Ag^+ cations was confirmed, indicating a shift in the equilibrium and a reservoir-like behavior of the functionalized sol−gels, continuously releasing Ag^+ cations that eventually reach toxic levels. No concentration range achieved bactericidal protection while maintaining the biocompatibility of the sol−gel coating. Instead, a time range was identified. Due to the time lag between the bactericidal and apoptotic actions, with *E. coli* exhibiting a killing time 8−18 times faster than fibroblasts, it becomes feasible to consider applications of silver-loaded sol−gel surfaces to significantly reduce the risk of infections and contaminations. While not suitable for implants, these coatings could be beneficial for materials with short-term or indirect skin contact, such as gloves. Surgical tools, doorknobs, or other items in high-risk areas such as operating rooms and hospital facilities could benefit from this type of a bactericidal coating.

■ ASSOCIATED CONTENT

Supporting Information

The Supporting Information is available free of charge at https://pubs.acs.org/doi/10.1021/acsomega.4c00726.

Extensive literature review; MIC/MBC determinations; microscopy and UV−visible determination of cytotoxicity toward NHDFs; ICP-AES data; LHD and MTT assays; and kinetics microscopic observation of cytotoxicity toward NHDFs (PDF)

■ AUTHOR INFORMATION

Corresponding Authors

Agathe Figarol − *Université Franche-Comté, CNRS, FEMTO-ST, F-25000 Besançon, France;* orcid.org/0000-0001-5121-3151; Email: agathe.figarol@femto-st.fr

Vincent Humblot − *Université Franche-Comté, CNRS, FEMTO-ST, F-25000 Besançon, France;* orcid.org/0000-0002-6266-3956; Email: vincent.humblot@femto-st.fr

Authors

Thibaut Zwingelstein − *Université Franche-Comté, CNRS, FEMTO-ST, F-25000 Besançon, France*

Vincent Luzet − *Université Franche-Comté, CNRS, FEMTO-ST, F-25000 Besançon, France*

Maude Crenna − *Centre Suisse d'Electronique et de Microtechnique CSEM SA, CH-2000 Neuchâtel, Switzerland*

Xavier Bulliard − *Centre Suisse d'Electronique et de Microtechnique CSEM SA, CH-2000 Neuchâtel, Switzerland*

Alba Finelli − *Centre Suisse d'Electronique et de Microtechnique CSEM SA, CH-2000 Neuchâtel, Switzerland*

Julien Gay − *Centre Suisse d'Electronique et de Microtechnique CSEM SA, CH-2000 Neuchâtel, Switzerland;* orcid.org/0000-0002-1270-5919

Xavier Lefèvre − *Centre Suisse d'Electronique et de Microtechnique CSEM SA, CH-2000 Neuchâtel, Switzerland*

Raphaël Pugin − *Centre Suisse d'Electronique et de Microtechnique CSEM SA, CH-2000 Neuchâtel, Switzerland*

Jean-François Laithier − *Coloral SA, 2088 Cressier, Switzerland*

Frédéric Chérioux − *Université Franche-Comté, CNRS, FEMTO-ST, F-25000 Besançon, France;* orcid.org/0000-0002-2906-0766

Complete contact information is available at: https://pubs.acs.org/10.1021/acsomega.4c00726

Author Contributions

Conceptualization: A.Fig., X.B., R.P., J.F.L., F.C., and V.H. Methodology: A.Fig., X.B., F.C., and V.H. Formal analyses: T.Z., A.Fig., X.B., F.C., and V.H. Investigation: T.Z., V.L., M.C., A.Fin., and X.L. Supervision: A.Fig., R.P., F.C., and V.H. The manuscript was written through contributions of all

https://doi.org/10.1021/acsomega.4c00726
ACS Omega 2024, 9, 24574−24583

authors. All authors have given approval to the final version of the manuscript.

Funding

The authors would like to thank the European cross-border cooperation program Interreg Franco-Suisse 2014−2020 and the FEDER agency (Fonds Européen de Développement Régional) for funding.

Notes

The authors declare no competing financial interest.

■ ACKNOWLEDGMENTS

The authors would like to thank Sylvaine Linget from Laboratoire QUALIO Analyses & Environnement for her help in the Ag release ICP-AES experiments with and without bacteria and Lorine Vacelet from Coloral SA for the Si release ICP-AES experiments. The authors would also like to thank Adeline Marguier and Fanny Lotthammer (FEMTO-ST) for preliminary experiments. This work was partly supported by the French RENATECH network and its FEMTO-ST technological facility.

■ REFERENCES

(1) Klasen, H. J. Historical Review of the Use of Silver in the Treatment of Burns. I. Early Uses. *Burns* **2000**, *26* (2), 117−130.

(2) Kędziora, A.; Wieczorek, R.; Speruda, M.; Matolínová, I.; Goszczyński, T. M.; Litwin, I.; Matolín, V.; Bugla-Płoskońska, G. Comparison of Antibacterial Mode of Action of Silver Ions and Silver Nanoformulations With Different Physico-Chemical Properties: Experimental and Computational Studies. *Front. Microbiol.* **2021**, *12*, No. 659614.

(3) Singh, R.; Rento, C.; Son, V.; Turner, S.; Smith, J. A. Optimization of Silver Ion Release from Silver-Ceramic Porous Media for Household Level Water Purification. *Water* **2019**, *11* (4), 816.

(4) Mishra, A.; Pradhan, D.; Halder, J.; Biswasroy, P.; Rai, V. K.; Dubey, D.; Kar, B.; Ghosh, G.; Rath, G. Metal Nanoparticles against Multi-Drug-Resistance Bacteria. *J. Inorg. Biochem.* **2022**, *237*, No. 111938.

(5) Ding, L.; Liu, Z.; Aggrey, M. O.; Li, C.; Chen, J.; Tong, L. Nanotoxicity: The Toxicity Research Progress of Metal and Metal-Containing Nanoparticles. *Mini-Rev. Med. Chem.* **2015**, *15* (7), 529−542.

(6) Sengul, A. B.; Asmatulu, E. Toxicity of Metal and Metal Oxide Nanoparticles: A Review. *Environ. Chem. Lett.* **2020**, *18* (5), 1659−1683.

(7) Bakhsheshi-Rad, H. R.; Ismail, A. F.; Aziz, M.; Akbari, M.; Hadisi, Z.; Khoshnava, S. M.; Pagan, E.; Chen, X. Co-Incorporation of Graphene Oxide/Silver Nanoparticle into Poly-L-Lactic Acid Fibrous: A Route toward the Development of Cytocompatible and Antibacterial Coating Layer on Magnesium Implants. *Mater. Sci. Eng., C* **2020**, *111*, No. 110812.

(8) Simchi, A.; Tamjid, E.; Pishbin, F.; Boccaccini, A. R. Recent Progress in Inorganic and Composite Coatings with Bactericidal Capability for Orthopaedic Applications. *Nanomedicine* **2011**, *7* (1), 22−39.

(9) Aksakal, B.; Demirel, M. In Vitro Study of Antimicrobial and Cell Viability on Newly Synthesized Bioglass-Based Bone Grafts: Effects of Selenium and Silver Additions. *Proc. Inst. Mech. Eng., Part H* **2018**, *232*, 1039−1047.

(10) Jaiswal, S.; Bhattacharya, K.; Sullivan, M.; Walsh, M.; Creaven, B. S.; Laffir, F.; Duffy, B.; McHale, P. Non-Cytotoxic Antibacterial Silver−Coumarin Complex Doped Sol−Gel Coatings. *Colloids Surf., B* **2013**, *102*, 412−419.

(11) Rahmani, M.; Moghanian, A.; Yazdi, M. S. The Effect of Ag Substitution on Physicochemical and Biological Properties of Sol-Gel Derived 60%SiO2−31%CaO−4%P2O5−5%Li2O (Mol%) Quaternary Bioactive Glass. *Ceram. Int.* **2021**, *47* (11), 15985−15994.

(12) Zhang, S.; Liang, X.; Gadd, G. M.; Zhao, Q. A Sol−Gel Based Silver Nanoparticle/Polytetrafluorethylene (AgNP/PTFE) Coating with Enhanced Antibacterial and Anti-Corrosive Properties. *Appl. Surf. Sci.* **2021**, *535*, No. 147675.

(13) Rojas, I. A.; Slunt, J. B.; Grainger, D. W. Polyurethane Coatings Release Bioactive Antibodies to Reduce Bacterial Adhesion. *J. Controlled Release* **2000**, *63* (1), 175−189.

(14) Chen, W.; Liu, Y.; Courtney, H. S.; Bettenga, M.; Agrawal, C. M.; Bumgardner, J. D.; Ong, J. L. In Vitro Anti-Bacterial and Biological Properties of Magnetron Co-Sputtered Silver-Containing Hydroxyapatite Coating. *Biomaterials* **2006**, *27* (32), 5512−5517.

(15) Song, W.-H.; Ryu, H. S.; Hong, S.-H. Antibacterial Properties of Ag (or Pt)-Containing Calcium Phosphate Coatings Formed by Micro-Arc Oxidation. *J. Biomed. Mater. Res., Part A* **2009**, *88A* (1), 246−254.

(16) Galandáková, A.; Franková, J.; Ambrožová, N.; Habartová, K.; Pivodová, V.; Zálešák, B.; Šafářová, K.; Smékalová, M.; Ulrichová, J. Effects of Silver Nanoparticles on Human Dermal Fibroblasts and Epidermal Keratinocytes. *Hum. Exp. Toxicol.* **2016**, *35* (9), 946−957.

(17) Hidalgo, E.; Domínguez, C. Study of Cytotoxicity Mechanisms of Silver Nitrate in Human Dermal Fibroblasts. *Toxicol. Lett.* **1998**, *98* (3), 169−179.

(18) Cortese-Krott, M. M.; Münchow, M.; Pirev, E.; Heβner, F.; Bozkurt, A.; Uciechowski, P.; Pallua, N.; Kröncke, K.-D.; Suschek, C. V. Silver Ions Induce Oxidative Stress and Intracellular Zinc Release in Human Skin Fibroblasts. *Free Radicals Biol. Med.* **2009**, *47* (11), 1570−1577.

(19) 14:00-17:00. *ISO 10993-5:2009*. ISO. https://www.iso.org/standard/36406.html (accessed March 04, 2024).

(20) Gaudillat, Q.; Krupp, A.; Zwingelstein, T.; Humblot, V.; Strohmann, C.; Jourdain, I.; Knorr, M.; Viau, L. Silver-Based Coordination Polymers Assembled by Dithioether Ligands: Potential Antibacterial Materials despite Received Ideas. *Dalton Trans.* **2023**, *52*, 5859.

(21) Ishida, T. Antibacterial Mechanism of Ag+ Ions for Bacteriolyses of Bacterial Cell Walls via Peptidoglycan Autolysins, and DNA Damages. *MOJ Toxicol.* **2018**, *4*, 345−350.

(22) International Organization for Standardization. *ISO - 11.100.20 - Biological Evaluation of Medical Devices; Standard ISO 10993*, 2022. https://www.iso.org/ics/11.100.20/x/ (accessed April 18, 2023).

(23) Sussman, E. M.; Casey, B. J.; Dutta, D.; Dair, B. J. Different Cytotoxicity Responses to Antimicrobial Nanosilver Coatings When Comparing Extract-Based and Direct-Contact Assays. *J. Appl. Toxicol.* **2015**, *35* (6), 631−639.

(24) Kawashita, M.; Tsuneyama, S.; Miyaji, F.; Kokubo, T.; Kozuka, H.; Yamamoto, K. Antibacterial Silver-Containing Silica Glass Prepared by Sol-Gel Method. *Biomaterials* **2000**, *21* (4), 393−398.

(25) Luo, S.-H.; Xiao, W.; Wei, X.-J.; Jia, W.-T.; Zhang, C.-Q.; Huang, W.-H.; Jin, D.-X.; Rahaman, M. N.; Day, D. E. *In Vitro* Evaluation of Cytotoxicity of Silver-Containing Borate Bioactive Glass. *J. Biomed. Mater. Res. B Appl. Biomater.* **2010**, *95B*, 441−448.

(26) Kaplan, A.; Akalin Ciftci, G.; Kutlu, H. M. The Apoptotic and Genomic Studies on A549 Cell Line Induced by Silver Nitrate. *Tumor Biol.* **2017**, *39* (4), No. 1010428317695033.

(27) Kristiansen, S.; Ifversen, P.; Danscher, G. Ultrastructural Localization and Chemical Binding of Silver Ions in Human Organotypic Skin Cultures. *Histochem. Cell Biol.* **2008**, *130* (1), 177−184.

(28) Zhan, D.; Li, X.; Nepomnyashchii, A. B.; Alpuche-Aviles, M. A.; Fan, F.-R. F.; Bard, A. J. Characterization of Ag+ Toxicity on Living Fibroblast Cells by the Ferrocenemethanol and Oxygen Response with the Scanning Electrochemical Microscope. *J. Electroanal. Chem.* **2013**, *688*, 61−68.

(29) Exner, M.; Bhattacharya, S.; Gebel, J.; Goroncy-Bermes, P.; Hartemann, P.; Heeg, P.; Ilschner, C.; Kramer, A.; Ling, M. L.; Merkens, W.; Oltmanns, P.; Pitten, F.; Rotter, M.; Schmithausen, R. M.; Sonntag, H.-G.; Steinhauer, K.; Trautmann, M. Chemical

https://doi.org/10.1021/acsomega.4c00726
ACS Omega 2024, 9, 24574−24583

Disinfection in Healthcare Settings: Critical Aspects for the Development of Global Strategies. *GMS Hyg. Infect. Control* **2020**, *15*, No. Doc36.

https://doi.org/10.1021/acsomega.4c00726
ACS Omega 2024, 9, 24574−24583